pling case, for it is generally agreed that for $U \approx \Gamma$ no particular subset of diagrams is dominant. Furthermore, having obtained a Kondo-like logarithmic divergence, it is not clear how to renormalize such that a well-behaved local moment susceptibility, consistent with experiment, results.

Hamann's scheme, less formalistic and perhaps on firmer ground than Keiter's in terms of physical insight, suffers from the two difficulties discussed in Sec. III; the extremal approximation to the y field does not appear to be as innocuous as previously thought, and the ND approximation may be only marginally adequate for the calculation of the d-state Green's function for the "time"-dependent problem.

The 2-field formalism without extremal approx-

imation thus appears to us to be the best framework for more powerful schemes. Furthermore, the limitations of the ND approximation can perhaps be overcome or shown to be unimportant. Although one can hope for a new breakthrough, for the present we must conclude that the FI method as applied to the Anderson model has proven more exotic than effective.

[1] P. W. Anderson, Phys. Rev. 124, 41 (1961).

[2] J. R. Schrieffer, lecture notes, Canadian Association of Physics, Summer School, Banff, 1969 (unpublished); and S. Q. Wang, W. E. Evenson, and J. R. Schrieffer, Phys. Rev. Letters 23, 92 (1969).

[3] J. R. Schrieffer, W. E. Evenson, and S. Q. Wang, Proceedings of the International Conference on Magnetism, Grenoble, 1970 (unpublished).

[4] H. Keiter, Phys. Rev. B 2, 3777 (1970).

[5] (a) D. R. Hamann, Phys. Rev. Letters 23, 95 (1969); (b) Phys. Rev. B 2, 1373 (1970).

[6] Reference 4, Sec. VI.

[7] J. Hubbard, Phys. Rev. Letters 3, 77 (1959).

[8] R. Bari, Phys. Rev. B 5, 2736 (1972).

[9] D. J. Amit, C. M. Bender, Phys. Rev. B 4, 3115 (1971).

[10] P. Nozières and C. DeDominicis, Phys. Rev. 178, 1097 (1969).

[11] G. Yuval and P. W. Anderson, Phys. Rev. B 1, 1522 (1970).

[12] P. W. Anderson, G. Yuval, and D. R. Hamann, Phys. Rev. B 1, 4464 (1970).

[13] See Ref. 5(b), Sec. VI B.

[14] See Ref. 5(b), Sec. IV B.

[15] K. D. Schotte and U. Schotte, Phys. Rev. B 4, 2228 (1971).

[16] J. R. Schrieffer (private communication).

[17] See Ref. 5(b), Ref. 22.

[18] D. J. Scalapino, Phys. Rev. Letters 16, 937 (1966).

[19] B. Kjöllerstrom, Phys. Status Solidi 43, 203 (1971).

Electron Distribution around a Magnetic Impurity in a Nonmagnetic Host*

P. Jena and D. J. W. Geldart
Department of Physics, Dalhousie University, Halifax, Nova Scotia, Canada
(Received 19 June 1972)

The spatial dependence of the electron density polarization per spin $\delta n^{\sigma}(r)$, produced by a magnetic ion in a nonmagnetic host, has been calculated in terms of the Friedel–Anderson model. The numerical results are found to be rather insensitive to variations of the model parameters describing the virtual bound state provided self-consistency is maintained. Our numerical results differ considerably, even in sign, from the well-known asymptotic form at first-nearest-neighbor distances and the asymptotic form is not adequate until $r \gtrsim 10k_F^{-1}$. An interpolation formula, incorporating lowest-order preasymptotic corrections, has also been given.

I. INTRODUCTION

It is well known that Mössbauer and nuclear-magnetic-resonance experiments probe local electronic spin and charge polarization at selected nuclear sites in alloys. The results of such experiments yield very sensitive tests of current theories of the electronic structure of alloys. For a brief review, we refer to the articles of Daniel and Friedel[1] and Blandin.[2] In almost all theoretical work to date, two assumptions have been made. First, the magnetic impurity ions are considered

to be sufficiently dilute so that their effects are additive. Thus, there is no correlation or interference between magnetic ions. Second, the change in electron density of spin σ induced by a single magnetic ion located at $\vec{r} = \vec{0}$ is assumed to be adequately represented by the asymptotic form, valid for sufficiently large r,

$$\delta n^\sigma(r) \simeq -\frac{5}{4\pi^2 r^3} \sin\delta_d^\sigma(\epsilon_F) \cos[2k_F r + \delta_d^\sigma(\epsilon_F)] \, , \quad (1)$$

where only the $l = 2$ or d-wave resonance is taken into account as we shall consider magnetic impurities of the $3d$ transition series. In Eq. (1), k_F is the Fermi wave number of the host metal and $\delta_d^\sigma(\epsilon_F)$ is the $l = 2$ phase shift for the scattering of electrons of spin σ at the Fermi energy.[1]

In this work, we consider the idealized limiting case of a *single* magnetic ion in a noble-metal host in order to avoid the question of correlations between magnetic ions. To be specific, we shall refer to a Mn ion in a Cu host.

Although the asymptotic form of $\delta n^\sigma(r)$ is valid for "sufficiently" large r, it is not obvious that the use of Eq. (1) is justified for the first few nearest-neighbor shells. This point can be quite significant for some problems because it is precisely the near-neighbor shells at which the induced polarization is largest and must therefore be treated accurately. In order to calculate $\delta n^\sigma(r)$ for these smaller values of r, it is necessary to specify the full wave-number and energy dependence of the conduction-electron scattering amplitude. Although the energy-shell scattering amplitude is essentially fixed by the Friedel sum rule

$$Z_d^\sigma = 5\delta_d^\sigma(\epsilon_F)/\pi \, , \quad (2)$$

the off-energy-shell scattering amplitude is sensitive to details of the electron wave functions and the bare impurity potential and can therefore be expected to be somewhat model dependent. Our objective has been the numerical calculation of $\delta n^\sigma(r)$ for three somewhat different, but reasonable, models for the electron-ion interaction. The encouraging conclusion which we have drawn is that the model dependence of the results is quite minimal provided physical self-consistency restrictions are maintained. On the other hand, the calculated results are found to differ not only in magnitude but also in *sign* from those predicted by use of the simple asymptotic form at the first-nearest-neighbor shells.

In Sec. II the required details of the calculation of $\delta n^\sigma(r)$ are formulated in terms of the Anderson model.[3] The models used for the d-wave-resonance scattering are specified in Sec. III and numerical results for the computed spin and charge polarizations are given in Sec. IV. Based on an analysis of the lowest-order preasymptotic correc-

tions to Eq. (1), we propose a simple interpolation formula for $\delta n^\sigma(r)$ in Sec. V which is reasonably accurate even at the first-nearest-neighbor distance. Finally, Sec. VI consists of a summary of our conclusions.

II. FORM OF $\delta n^\sigma(r)$ IN ANDERSON MODEL

Our calculation of the charge and spin polarization due to a $3d$ impurity is based on Anderson's degenerate-added-orbital model and is carried out in the Hartree−Fock approximation.[3] The corresponding Hamiltonian is

$$\mathcal{H} = \sum_{\vec{k}\sigma} \epsilon_{\vec{k}}^\sigma C_{\vec{k}\sigma}^\dagger C_{\vec{k}\sigma} + \sum_m \epsilon_{d0}^\sigma C_{dm\sigma}^\dagger C_{dm\sigma}$$

$$+ \sum_{\vec{k}m\sigma} (V_{\vec{k}dm} C_{\vec{k}\sigma}^\dagger C_{dm\sigma} + V_{dm\vec{k}} C_{dm\sigma}^\dagger C_{\vec{k}\sigma}) \, . \quad (3)$$

The notation is standard. The host conduction-band ($4S$) energies will be taken to be $\hbar^2 k^2/2m$, the localized-state energies ϵ_{d0}^σ will be specified later in this section, and the mixing matrix element is

$$V_{\vec{k}dm} = \int d^3r \, B_{\vec{k}}^*(\vec{r}) v(\vec{r}) \Phi_{dm}(\vec{r}) \, . \quad (4)$$

The average effective potential is taken to be of screened Coulomb form and spherically symmetrical:

$$v(\vec{r}) = Z^* e^2 e^{-q_{TF}r}/r \quad , \quad (5)$$

where Z^* is an "effective" charge of the impurity ion and q_{TF} is taken as the Thomas−Fermi screening constant. The wave function describing the resonance is basically a $l = 2$ atomic function,

$$\phi_{dm}(\vec{r}) \propto r^2 e^{-\lambda r} Y_{2m}(\hat{r}) \, , \quad (6a)$$

where λ is chosen to fit approximately the form factor of a Mn ion. However, to avoid an over-complete set of functions in the range of conduction-electron energies, the atomic function should be orthogonalized to the host Bloch functions so that[4,5]

$$\Phi_{dm}(\vec{r}) = \left(\phi_{dm}(\vec{r}) - \sum_{\vec{k}} B_{\vec{k}}(\vec{r}) \langle B_{\vec{k}} | \phi_{dm} \rangle \right) \nu_d \, , \quad (6b)$$

where the normalization constant

$$\nu_d = \left(1 - \sum_{\vec{k}} |\langle B_{\vec{k}} | \phi_{dm} \rangle|^2 \right)^{-1/2} \, .$$

With the set of functions $\{\Phi_{dm}, B_{\vec{k}}\}$ taken as a basis, the electron density of spin σ at the point $\vec{r}$ (measured from the Mn ion at the origin) is given by

$$n^\sigma(\vec{r}) = n_{dd}^\sigma(\vec{r}) + n_{dB}^\sigma(\vec{r}) + n_{Bd}^\sigma(\vec{r}) + n_{BB}^\sigma(\vec{r}) \, , \quad (7)$$

where the various terms are given by

$$n_{dd}^\sigma(\vec{r}) = \sum_m \Phi_{dm}^*(\vec{r}) \Phi_{dm}(\vec{r}) \langle C_{dm\sigma}^\dagger C_{dm\sigma} \rangle \, , \quad (8a)$$

$$n_{dB}^\sigma(\vec{r}) = \sum_{m\vec{k}} \Phi_{dm}^*(\vec{r}) B_{\vec{k}}(\vec{r}) \langle C_{dm\sigma}^\dagger C_{\vec{k}\sigma} \rangle \, , \quad (8b)$$
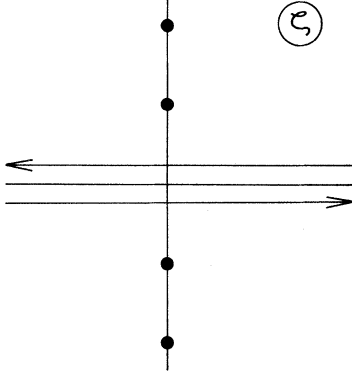
FIG. 1. Contour in the ζ plane for the integral in Eq. (9). Dots indicate the poles of the Fermi function $f(\zeta)$.

$$n^{\sigma}_{Bd}(\vec{r}) = \sum_{\vec{k}m} B^{*}_{\vec{k}}(\vec{r})\Phi_{dm}(\vec{r})\langle C^{\dagger}_{\vec{k}\sigma}C_{dm\sigma}\rangle , \qquad (8c)$$

$$n^{\sigma}_{BB}(\vec{r}) = \sum_{\vec{k},\vec{k}'} B^{*}_{\vec{k}}(\vec{r})B_{\vec{k}'}(\vec{r})\langle C^{\dagger}_{\vec{k}'\sigma}C_{\vec{k}\sigma}\rangle . \qquad (8d)$$

The procedure for expressing these densities in terms of the propagator for electrons in the localized state is known,[3] so only some results will be quoted. For example,

$$n^{\sigma}_{dd}(\vec{r}) = \sum_{m}\Phi_{dm}(\vec{r})\Phi^{*}_{dm}(\vec{r})\int \frac{d\zeta}{2\pi i} G^{\sigma}_{dd}(\zeta)f(\zeta) \qquad (9a)$$

and

$$n^{\sigma}_{BB}(\vec{r}) = \sum_{\vec{k}\vec{k}'} B^{*}_{\vec{k}'}(\vec{r})B_{\vec{k}}(\vec{r})\int \frac{d\zeta}{2\pi i} f(\zeta)G^{\sigma}_{\vec{k}\vec{k}'}(\zeta) , \qquad (9b)$$

where

$$G^{\sigma}_{dd}(\zeta) = [\zeta - \epsilon^{\sigma}_{d0} - \Sigma^{\sigma}_{d}(\zeta)]^{-1} \qquad (10a)$$

and

$$G^{\sigma}_{\vec{k}\vec{k}'}(\zeta) = \frac{\delta_{\vec{k}\vec{k}'}}{\zeta - \epsilon^{\sigma}_{\vec{k}}} + \frac{T^{\sigma}_{\vec{k}\vec{k}'}(\zeta)}{(\zeta - \epsilon^{\sigma}_{\vec{k}})(\zeta - \epsilon^{\sigma}_{\vec{k}'})} . \qquad (10b)$$

The contour of the ζ integration is shown in Fig. 1 and $f(\zeta)$ denotes the usual Fermi function. Although our numerical results are given for the $T \to 0$ limit, the finite-temperature formalism is convenient for motivating the transformations of integrals described in Sec. IV. In Eq. (10), $\Sigma^{\sigma}_{d}(\zeta)$ is the usual mixing self-energy

$$\Sigma^{\sigma}_{d}(\zeta) = \sum_{\vec{k}} \frac{|V_{\vec{k}dm}|^{2}}{\zeta - \epsilon^{\sigma}_{\vec{k}}} , \qquad (11)$$

and the T matrix for band-electron scattering is

$$T^{\sigma}_{\vec{k}\vec{k}'}(\zeta) = \sum_{m} V_{\vec{k}dm}G^{\sigma}_{dd}(\zeta)V_{dm\vec{k}'} . \qquad (12)$$

The major self-consistency requirement to be imposed on this calculation is the Friedel sum rule. To see how this constrains parameters, write Eq. (7) as $n_{0}(r) + \delta n^{\sigma}(r)$, where the "unperturbed" Bloch-electron density is given by the first term on the

right-hand side of Eq. (10b). Since the basis functions are orthonormal, the net change in the electron density when integrated over the volume of the crystal

$$Z^{\sigma}_{d} = \int d^{3}r \, \delta n^{\sigma}(\vec{r}) \qquad (13a)$$

is contributed only by Eqs. (8a) and (8d) and is seen to satisfy

$$Z^{\sigma}_{d} = 5\int d\zeta f(\zeta)\frac{\partial}{\partial\zeta}\ln[\zeta - \epsilon^{\sigma}_{d0} - \Sigma^{\sigma}_{d}(\zeta)] = \frac{5}{\pi}\delta^{\sigma}_{d}(\epsilon_{F}) . \qquad (13b)$$

The phase shift, in analogy with the usual scattering theory, is defined in the limit $\zeta = \epsilon + i0^{+}$ by

$$-G_{dd}(\epsilon + i0^{+}) = e^{i\delta^{\sigma}_{d}(\epsilon)}/\{[\epsilon - \epsilon^{\sigma}_{d0} - \Delta^{\sigma}_{d}(\epsilon)]^{2} + \Gamma^{\sigma}_{d}(\epsilon)^{2}\}^{1/2} \qquad (14)$$

and real and imaginary parts of the self-energy have been separated by

$$\Sigma^{\sigma}_{d}(\epsilon + i0^{+}) = \Delta^{\sigma}_{d}(\epsilon) - i\Gamma^{\sigma}_{d}(\epsilon) . \qquad (15)$$

Now a fully self-consistent treatment of the magnetic ion would require the solution of a set of complex coupled equations to determine even the existence of spin splitting in terms of the basic parameters of the Anderson model (Coulomb and exchange integrals, mixing matrix elements, and so on). In view of the many uncertainties in the precise details of the problem, we adopted a simplified procedure. We wish to describe situations which are known to be spin split, so $Z^{\dagger}_{d} \neq Z^{\dagger}_{d}$ was assumed at the outset. The two spin levels were then treated completely *independently* in much the same spirit as in early work of Friedel and others.[1,2] That is, reasonable values of $Z^{\dagger}_{d}$ and $Z^{\dagger}_{d}$ are specified by the screening condition $(Z^{\dagger}_{d} + Z^{\dagger}_{d})$ and the experimentally known magnetic moment $[\propto(Z^{\dagger}_{d} - Z^{\dagger}_{d})]$. From Eqs. (13b) and (14), this determines $\delta^{\sigma}_{d}(\epsilon_{F})$. Since $\Delta^{\sigma}_{d}(\epsilon_{F})$ and $\Gamma^{\sigma}_{d}(\epsilon_{F})$ are fixed already by the band structure of the host and the strength of the mixing interaction, self-consistency for each spin is imposed by finally choosing the parameters ϵ^{σ}_{d0} to satisfy

$$\sin\delta^{\sigma}_{d}(\epsilon_{F}) = \Gamma^{\sigma}_{d}(\epsilon_{F})/\{[\epsilon_{F} - \epsilon^{\sigma}_{d0} - \Delta^{\sigma}_{d}(\epsilon_{F})]^{2} + \Gamma^{\sigma}_{d}(\epsilon_{F})^{2}\}^{1/2} , \qquad (15a)$$

$$\cos\delta^{\sigma}_{d}(\epsilon_{F}) = -[\epsilon_{F} - \epsilon^{\sigma}_{d0} - \Delta^{\sigma}_{d}(\epsilon_{F})]/\{[\epsilon_{F} - \epsilon^{\sigma}_{d0} - \Delta^{\sigma}_{d}(\epsilon_{F})]^{2} + \Gamma^{\sigma}_{d}(\epsilon_{F})^{2}\}^{1/2} , \qquad (15b)$$

so as to reproduce the Z^{σ}_{d} required by Eq. (13b). By simplifying the self-consistency problem in this way, we maintain the simplicity and intuitive appeal of Friedel's approach while still quantitatively treating the wave-number and energy dependence of the scattering within the spirit of Anderson's model.

At this point the basic features of the formalism are established so some simplifications of wave functions will be made. We require the electron

density only at lattice sites occupied by host ions. At such points,

$$B_{\vec{k}}(\vec{r}) = e^{i\vec{k}\cdot\vec{r}} B_{\vec{k}}(0) \ , \qquad (16a)$$

and $B_{\vec{k}}(0)$ will be approximated by a plane wave orthogonalized to the occupied wave functions of a single ion core. Thus, *at lattice points*,

$$B_{\vec{k}}(\vec{r}) \simeq \frac{e^{i\vec{k}\cdot\vec{r}}}{\Omega^{1/2}} \left(1 - \sum_{nlm}^{occ} b_{nlm}(\vec{k})\Psi_{nlm}(0)\right)\nu_k = \frac{e^{i\vec{k}\cdot\vec{r}}}{\Omega^{1/2}}\,\alpha \ , \tag{16b}$$

where ν_k is the normalization constant and Ω is the crystal volume. Thus, the Bloch-wave enhancement is roughly incorporated by

$$\alpha \cong \left(1 - \sum_{n} b_{n00}(k_F)\Psi_{n00}(0)\right)\nu_F \ . \tag{16c}$$

Thus no attempt is made to include detailed structure of the Bloch functions and this approximation will be used for the Bloch functions which enter explicitly in Eqs. (8). For example, subtracting the unperturbed Bloch-wave contribution, Eq. (8d) becomes

$$\delta n_{BB}^{\sigma}(\vec{r}) \simeq \alpha^2 \sum_{\vec{k}\vec{k}'} \frac{e^{i(\vec{k}-\vec{k}')\cdot\vec{r}}}{\Omega} \int \frac{d\zeta}{2\pi i} f(\zeta) \frac{T_{\vec{k}\vec{k}'}^{\sigma}(\zeta)}{(\zeta - \epsilon_{\vec{k}}^{\sigma})(\zeta - \epsilon_{\vec{k}'}^{\sigma})} \ . \tag{17}$$

Note, however, that Bloch functions are still required in the calculation of the matrix elements which enter the scattering amplitude. With this exception, the calculation is reduced to an electron-gas problem. In the same way, a single factor of α appears in each of Eqs. (8b) and (8c).

As a further simplification, $\Phi_{dm}(\vec{r}) \simeq \phi_{dm}(\vec{r})$ will be used in subsequent calculations. This is justified by their large overlap. Thus, from Eq. (6),

$$\langle \phi_{dm} | \Phi_{dm} \rangle = \left(1 - \sum_{\vec{k}} |\langle B_{\vec{k}} | \phi_{dm}\rangle|^2\right)^{1/2} \ . \tag{18}$$

If the Cu $3d$ core functions are also approximated by the analytic form of Eq. (6a) with an appropriate λ_0, slightly larger (by about 20%) than that required for the more extended Mn core functions,[6] the sum in (18) can easily be estimated. In Appendix A it is shown that the overlap integral is about 96%.

Finally, it can be shown that only $\delta n_{BB}^{\sigma}(r)$ contributes significantly to $\delta n^{\sigma}(r)$ for values of $r \geq a_{nn}$, the nearest-neighbor distance. The fact that $n_{dd}^{\sigma}(r)$, $n_{dB}^{\sigma}(r)$, and $n_{Bd}^{\sigma}(r)$ are all negligible for $r \geq a_{nn}$ follows from the very small overlap of the Mn core functions even at nearest-neighbor distances. This is shown in detail in Appendix B.

The net result of these approximations and estimates is that the charge density at host lattice sites is given by Eq. (17) only. Our main objective in the present work has been the study of how the wave-number and energy dependence of $T_{\vec{k}\vec{k}'}^{\sigma}(\zeta)$, which is still quite complicated, influences the amplitude and phase of $\delta n^{\sigma}(r)$. In Sec. III, we

discuss three different models for the mixing matrix elements and localized-state self-energy.

III. MODELS FOR RESONANCE SCATTERING

In this section we shall discuss various models to study the resonant scattering amplitude of conduction electrons from a single magnetic impurity ion. The purpose of this is to assess the sensitivity of the resulting resonance line shape to the choice of the model parameters. Care is taken to satisfy self-consistency criteria, discussed in Sec. II, within the framework of the model. The various models differ from each other by virture of the approximations made to evaluate the matrix element of the mixing potential $V_{\vec{k}d}$, the conduction-band state density $N(\epsilon)$, and the frequency dependence of the self-energy terms $\Sigma_d^{\sigma}(\epsilon + i0^+) = \Delta_d^{\sigma}(\epsilon) - i\Gamma_d^{\sigma}(\epsilon)$. We consider three models: (A) orthogonalized-plane-wave (OPW) model, (B) finite-bandwidth (FBW) model, and (C) constant-self-energy (CSE) model.

A. Orthogonalized-Plane-Wave Model

In this model, the conduction-band states are taken as Bloch waves which are obtained by orthogonalizing the plane-wave states to the outermost $3d$ states of the host Cu ion. In principle, an OPW should be constructed by orthogonalizing the plane-wave states to all the occupied core states of the host ion. However, since the inner core states are much more localized than the $3d$ states, the overlap of the $3d$ states with the plane waves is much greater, and to a fair degree of accuracy, we can consider the Bloch state simply to be a single OPW. Since it is the $3d$ components which are important for the mixing matrix elements, we shall take

$$B_{\vec{k}}(\vec{r}) \simeq \Omega^{-1/2}\left(e^{i\vec{k}\cdot\vec{r}} - \sum_{m} b_{dm}(\vec{k})\Psi_{dm}(\vec{r})\right)\nu_k \ . \tag{19}$$

The m sum runs over the five azimuthal quantum numbers corresponding to the $d(l=2)$ states. The overlap integral $b_{dm}(\vec{k})$ is defined by

$$b_{dm}^*(\vec{k}) \equiv \int d^3r \, e^{-i\vec{k}\cdot\vec{r}} \Psi_{dm}(\vec{r}) = -4\pi Y_{2m}(\hat{k})\,a_{kd} \ , \tag{20}$$

where

$$a_{kd} \equiv \int_0^{\infty} dr \, r^2 j_2(kr)\psi_d(r) \tag{21a}$$

and

$$\Psi_{dm}(\vec{r}) = \psi_d(r) Y_{2m}(\hat{r}) \ . \tag{21b}$$

As discussed in Sec. II, we take

$$\psi_d(r) = A_0 r^2 e^{-\lambda_0 r} \ , \tag{22a}$$

where the parameter λ_0 is obtained by fitting to the Cu ion $3d$ form factors. The normalization constant A_0 is found easily to be

$$A_0 = \left(\tfrac{8}{45}\lambda_0^7\right)^{1/2} \ . \tag{22b}$$

Substituting Eq. (22a) in Eq. (21), we get

$$a_{kd} = A_0 \frac{48\lambda_0 k^2}{(\lambda_0^2 + k^2)^4} \quad . \tag{23}$$

With the choice of the above OPW basis function, the matrix elements of the potential $v(\vec{r})$ can now be calculated.

Using these results in Eq. (4), we have

$$V_{\vec{k}dm} = -\frac{4\pi}{\Omega^{1/2}} Y_{2m}(\hat{k}) (I_{dk} - J_{dk}) \nu_k \, , \tag{24a}$$

with

$$I_{dk} = \frac{8 Z^* e^2 A k^2}{[k^2 + (q_{TF} + \lambda)^2]^3} \tag{24b}$$

and

$$J_{dk} = \frac{1024 Z^* e^2 A k^2 \lambda^8}{(\lambda^2 + k^2)^4 (2\lambda + q_{TF})^6} \quad . \tag{24c}$$

In Eqs. (24), the λ parameters for both Mn and Cu ions have been taken to be the same since, as noted in Sec. II, they differ by only 20%. As will be seen in Sec. IV, the results for $\delta n^s(r)$ are insensitive to variations in λ. It is interesting to compare the relative magnitudes of J_{dk} and I_{dk}:

$$\frac{J_{dk}}{I_{dk}} = 128 \frac{\lambda^8 [k^2 + (q_{TF} + \lambda)^2]^3}{(k^2 + \lambda^2)^4 (2\lambda + q_{TF})^6} \quad . \tag{25a}$$

In the present calculation, k_F, q_{TF}, and λ were taken to be $0.741 a_0^{-1}$, $0.971 a_0^{-1}$, and $2.50 a_0^{-1}$, respectively. Thus,

$$J_{dk}/I_{dk}(k \to 0) \simeq 4.9 \tag{25b}$$

and

$$J_{dk}/I_{dk}(k \to k_F) \simeq 4.0 \, . \tag{25c}$$

This clearly demonstrates the importance of the core contribution to the strength of scattering. Its importance will be discussed later while considering the width of the resonance.

In the subsequent analysis, we shall neglect the normalization factor ν_k. From Eq. (19), it can easily be verified that ν_k is almost unity and much more slowly varying for $k \sim k_F$ than other factors in Eqs. (24). To be specific, $\nu_F \sim 1.03$, while $\nu_F' \sim 0.9/k_F$. The omission of the corrections due to ν_k greatly simplifies the calculation of the d-state self-energy and, according to the discussion in Sec. IV, is not expected to influence $\delta n^s(r)$ significantly.

In the limit of a vanishingly small concentration of impurities, any induced spin splitting of the conduction band is negligible. Then $\Delta_{dm}(\epsilon)$ and $\Gamma_{dm}(\epsilon)$ are independent of spin direction. From Eq. (14),

$$\Gamma_{dm}(\epsilon) = \pi \sum_{\vec{k}} |V_{\vec{k}dm}|^2 \delta(\epsilon - \epsilon_k) \, . \tag{26a}$$

Using Eq. (24a), we have

$$\Gamma_{dm}(\epsilon) = 4\pi^2 N_0(\epsilon) [I_{dk} - J_{dk}]_\epsilon^2 \, . \tag{26b}$$

The electron density of states is taken to be that of a free-electron system, $N_0(\epsilon)$, and the square bracket in Eq. (26b) has to be evaluated at energy ϵ:

$$N_0(\epsilon) = mk/2\hbar^2 \pi^2 \, . \tag{27}$$

The evaluation of the real part of the self-energy,

$$\Delta_{dm}(\epsilon) = \mathcal{P} \sum_{\vec{k}} \frac{|V_{\vec{k}dm}|^2}{\epsilon - \epsilon_k} \, , \tag{28}$$

where $\mathcal{P}$ denotes that the principal value is to be taken, is rather lengthy but straightforward. We have therefore chosen to give only the final steps. Using Eq. (24a), Eq. (28) can be written as a sum of three terms which represents the contributions of the plane-wave–plane-wave, plane-wave–core, and core-core terms. Thus

$$\Delta_{dm}(\epsilon) = \Delta_{dm}^I(\epsilon) + \Delta_{dm}^{II}(\epsilon) + \Delta_{dm}^{III}(\epsilon) \, , \tag{29a}$$

with

$$\Delta_{dm}^I(\epsilon) \equiv 4\pi \, \mathcal{P} \int_0^\infty d\epsilon_k I_{dk}^2 \frac{N_0(\epsilon_k)}{\epsilon - \epsilon_k}$$

$$= \frac{e^4}{4} \left(\frac{\hbar^2}{2m}\right)^{5/2} \frac{(Z^* A)^2}{\epsilon_I^{5/2}(\epsilon_I + \epsilon)^6} (-3\epsilon_I^5 - 25\epsilon_I^4 \epsilon - 150\epsilon_I^3 \epsilon^2 + 150\epsilon_I^2 \epsilon^3 + 25\epsilon_I \epsilon^4 + 3\epsilon^5) \, , \tag{29b}$$

$$\Delta_{dm}^{II}(\epsilon) \equiv -8\pi \mathcal{P} \int_0^\infty d\epsilon_k I_{dk} J_{dk} \frac{N_0(\epsilon_k)}{\epsilon - \epsilon_k}$$

$$= \frac{e^4}{4} \left(\frac{\hbar^2}{2m}\right)^{5/2} (64 Z^* A)^2 \frac{\epsilon_0^{9/2}}{\epsilon^3}$$

$$\times \left(\frac{\epsilon_0^3 + 5\epsilon_0^2 \epsilon + 15\epsilon_0 \epsilon^2 - 5\epsilon^3}{\epsilon_0(\epsilon_I + \epsilon)^3 (\epsilon_0 + \epsilon)^4} + \frac{-5\epsilon_I^3 - 4\epsilon_I^{5/2} \epsilon_0^{1/2} + 9\epsilon_I^2 \epsilon_0 + 8\epsilon_I^{3/2} \epsilon_0^{3/2} - 3\epsilon_I \epsilon_0^2 - 4\epsilon_0^{5/2} - \epsilon_0^3}{\epsilon_0(\epsilon_I - \epsilon_0)^2 (\epsilon_I + \epsilon)^3 (\epsilon_I^{1/2} + \epsilon_0^{1/2})^4}\right)$$

$$-\frac{5(\epsilon_I^{5/2} - \epsilon_I^2\epsilon_0^{1/2} - 2\epsilon_I^{3/2}\epsilon_0 + 2\epsilon_I\epsilon_0^{3/2} + \epsilon_I^{1/2}\epsilon_0^2 - \epsilon_0^{5/2})}{\epsilon_0(\epsilon_I - \epsilon_0)^3(\epsilon_I^{1/2} + \epsilon_0^{1/2})^5(\epsilon_I + \epsilon)}\Biggr) \,, \qquad (29c)$$

and, finally,

$$\Delta_{dm}^{III}(\epsilon) \equiv 4\pi \mathcal{P} \int_0^\infty d\epsilon_k J_{dk}^2 \frac{N_0(\epsilon_k)}{\epsilon - \epsilon_k}$$

$$= \frac{e^4}{4}\left(\frac{\hbar^2}{2m}\right)^{5/2} \frac{(64 Z^*A)^2 \epsilon_0^{7/2}}{2\tilde{\epsilon}^6(\epsilon_0 + \epsilon)^8}$$

$$\times (-9\epsilon_0^7 - 105\epsilon_0^6\epsilon - 1040\epsilon_0^5\epsilon^2 + 1575\epsilon_0^4\epsilon^3 + 525\epsilon_0^3\epsilon^4 + 189\epsilon_0^2\epsilon^5 + 45\epsilon_0\epsilon^6 + 5\epsilon^7) \,. \qquad (29d)$$

The parameters ϵ_I, ϵ_0, and $\tilde{\epsilon}$ in the above equations are defined as

$$\epsilon_I \equiv (\hbar^2/2m)(q+\lambda)^2 \,, \qquad \epsilon_0 \equiv (\hbar^2/2m)(\lambda)^2 \,, \qquad \tilde{\epsilon} \equiv (\hbar^2/2m)(q+2\lambda)^2 \,. \qquad (29e)$$

The spectral function can now be given by

$$A_d^\sigma(\epsilon) = \frac{1}{\pi} \frac{\Gamma_d(\epsilon)}{[\epsilon - \epsilon_{d0}^\sigma - \Delta_d(\epsilon)]^2 + \Gamma_d(\epsilon)^2} \,. \qquad (30)$$

The determination of ϵ_{d0}^σ via Eq. (15) has been outlined in Sec. II and it is through this parameter that the self-consistency criterion, Eq. (13b), is satisfied. The only unspecified parameter in the theory is Z^* and its value is chosen so that (i) the charge-neutrality condition, Eq. (13b), is satisfied and (ii) the resonance in Eq. (30) is "reasonably" broad. We also imposed the weaker condition that (iii) the resonance spectral function should reflect the true enhancement in state density by requiring that

$$Z_d^{*\sigma} = 5 \int d\epsilon \, f(\epsilon) A_d^\sigma(\epsilon)$$

be approximately the same as Z_d^σ. For this model, $Z^* \simeq 2$ was found to satisfy these three require-

ments. It must be pointed out that these conditions could not be simultaneously satisfied by using only plane waves (rather than OPW) to evaluate matrix elements of the potential.

Having specified the remaining parameter Z^*, the properties of the resonance are uniquely determined for each value of Z_d^σ. In Fig. 2, we have plotted the parameter ϵ_{d0}^σ as a function of Z_d^σ to illustrate its dependence on the screening charge per spin. In Fig. 3, the spectral functions corresponding to $Z_d^\sigma = 0.5$ and 4.5, respectively, are given. Note that the positions and the widths of the resonance are as expected from general physical considerations.

In order to verify the relative insensitivity of these results to details of the OPW model, we shall also consider two alternative and simpler models.

B. Finite-Bandwidth Model

As was previously pointed out, the use of plane waves and a free-electron state density does not yield a consistent spectral function of the desired
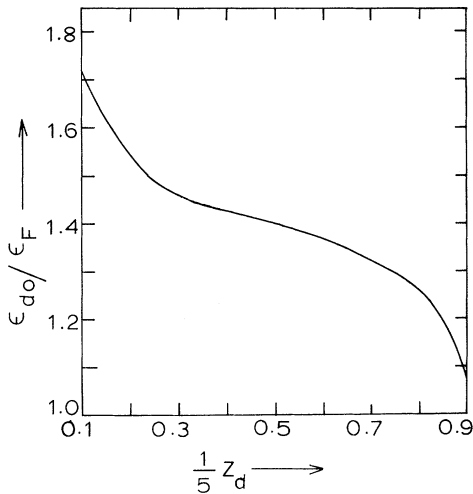

FIG. 2. Variation of the unperturbed d-state energy ϵ_{d0}^σ with self-consistent final occupation Z_d^σ as required by the Friedel sum rule in the OPW model.
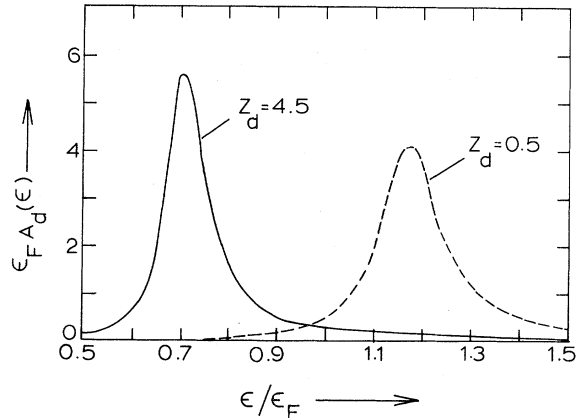

FIG. 3. Spectral functions $A_d^\sigma(\epsilon)$ for $Z_d^\sigma = 0.5$ and 4.5 in the OPW model.

width. The reason is that there are large contributions to $\Delta_d(\epsilon)$, Eqs. (29), from the high-energy region where $N_0(\epsilon)$ is large. On the other hand, for the range of energies of interest ($\epsilon \sim \epsilon_F$), the free-electron band may be adequate for $\Gamma_d(\epsilon)$, Eq. (26b). This suggests, if plane waves are to be used as basis functions in a simplified model, that a more "realistic" state density must be used. To simulate a state density of finite bandwidth, we have chosen

$$N(\epsilon) = \frac{\epsilon^{5/2}}{4\pi(I_{dk})^2} \frac{C\epsilon_F^8}{(\epsilon + \epsilon_F)^8} , \qquad (31)$$

where the constant C is given by

$$C = \frac{(16 Z^* A)^2 2^8}{\pi(\epsilon_F + \epsilon_I)^8} , \qquad (32)$$

so that $N(\epsilon_F) = N_0(\epsilon_F)$. With this choice of state density, $N(\epsilon) \sim \epsilon^{1/2}$ for small ϵ and $N(\epsilon) \sim \epsilon^{-3/2}$ for large ϵ. Furthermore, this particular form of $N(\epsilon)$ leads to a simple analytic form for $\Delta_d(\epsilon)$. From Eq. (28) we easily obtain

$$\Gamma_d(\epsilon) = 4\pi^2 N(\epsilon)[I_{dk}^2]_\epsilon . \qquad (33)$$

Also,

$$\Delta_d(\epsilon) = 4\pi \mathscr{P} \int_0^\infty d\epsilon_k I_{dk}^2(\epsilon_k) \frac{N(\epsilon_k)}{\epsilon - \epsilon_k}$$

$$= \frac{e^4}{4} \left(\frac{\hbar^2}{2m}\right)^{5/2} \frac{32(Z^* A)^2}{(\epsilon_F + \epsilon_I)^8} \frac{\epsilon_F^{7/2}}{(\epsilon + \epsilon_F)^8}$$

$$\times (-9\epsilon_F^7 - 105\epsilon_F^6 \epsilon - 945\epsilon_F^5 \epsilon^2 + 1575\epsilon_F^4 \epsilon^3 + 525\epsilon_F^3 \epsilon^4 + 189\epsilon_F^2 \epsilon^5 + 45\epsilon_F \epsilon^6 + 5\epsilon^7) . \qquad (34)$$

For this FBW model, we find that the three consistency requirements mentioned previously are well satisfied for $Z^* \simeq 5$. The resulting spectral functions for $Z_d^\sigma = 0.5$ and 4.5, respectively, are plotted in Fig. 4 and are seen to be similar to those of the OPW model.

C. Constant-Self-Energy Model

In the simplest model of all, the energy dependence of $\Gamma_d(\epsilon)$ and $\Delta_d(\epsilon)$ is completely neglected.[7] To obtain a reasonable width, we take[1]

$$\Gamma_d(\epsilon) = \Gamma_d \simeq \tfrac{1}{6} \epsilon_F . \qquad (35)$$

Specifying Z_d^σ then determines

$$E_d^\sigma = \epsilon_{d0}^\sigma + \Delta_d \qquad (36a)$$

in terms of Γ_d. Using Eq. (15),

$$E_d^\sigma - \epsilon_F = \Gamma_d / \tan\delta_d^\sigma(\epsilon_F) . \qquad (36b)$$

This choice yields the usual Lorentzian form for the resonance, which is again similar to the previous forms. In Sec. IV we describe the calculation of $\delta n^\sigma(r)$ and shall see how sensitively it depends on the choice of the resonance spectrum.

IV. NUMERICAL RESULTS FOR $\delta n^\sigma(r)$

From Eq. (12), we see that the T matrix required for $\delta n^\sigma(r)$ is a sum of separable terms, so the $\vec{k}$ and $\vec{k}'$ sums in Eq. (17) can be evaluated independently. Since the angular dependence of $V_{\vec{k}dm}$ is given by $Y_{2m}(\hat{k})$, we easily find

$$\sum_{\vec{k}} \frac{e^{i\vec{k}\cdot\vec{r}}}{\Omega^{1/2}} \frac{V_{\vec{k}dm}}{\zeta - \epsilon_k} = F_r(\zeta) Y_{2m}(\hat{r}) \qquad (37a)$$

on integrating over the angles of $\vec{k}$. Similarly,

$$\sum_{\vec{k}} \frac{e^{-i\vec{k}'\cdot\vec{r}}}{\Omega^{1/2}} \frac{V_{dm\vec{k}'}}{\zeta - \epsilon_{k'}} = F_r(\zeta) Y_{2m}^*(\hat{r}) . \qquad (37b)$$

Of course, the form of $F_r(\zeta)$ depends on the model chosen. Details of the calculations will now be given for the OPW model and modifications required to apply to the FBW and CSE models will be indicated later.

In the OPW model, it follows from Eqs. (24a) and (37) that

$$F_r(\zeta) = \frac{2}{\pi} \int_0^\infty dk \, k^2 j_2(kr) \frac{I_{dk} - J_{dk}}{\zeta - \epsilon_k} . \qquad (38)$$

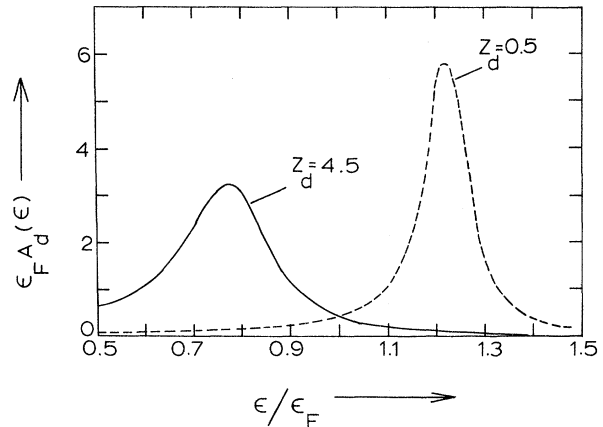Inserting (37) into Eq. (17) and carrying out the

FIG. 4. Spectral functions $A_d^\sigma(\epsilon)$ for $Z_d^\sigma = 0.5$ and 4.5 in the FBW model.

sum over the azimuthal quantum number results in

$$\delta n^{\sigma}(r) = \frac{5\alpha^2}{4\pi} \int \frac{d\zeta}{2\pi i} \, f(\zeta) F_r^2(\zeta) G_{dd}^{\sigma}(\zeta) \; . \qquad (39)$$

In our numerical work, we found it convenient to transform Eq. (39) by distorting the contour of integration to pick up only the discrete poles of the Fermi function at $\zeta = \epsilon_F + i\omega_n$, where $\omega_n = (2n + 1)\pi k_B T$. In the limit of low T, the sum over ω_n is replaced by an integral. Then

$$\delta n^{\sigma}(r) = \frac{5\alpha^2}{4\pi^2} \, \mathrm{Re} \, Q^{\sigma}(r) \; , \qquad (40a)$$

where

$$Q^{\sigma}(r) = \int_0^{\infty} d\omega \, F_r^2(\epsilon_F + i\omega) G_{dd}^{\sigma}(\epsilon_F + i\omega) \; . \qquad (40b)$$

The explicit form of $F_r(\epsilon_F + i\omega)$ required in Eq. (40b) can be obtained by converting Eq. (38) to a contour integral in the complex k plane. Using Eqs. (24b) and (24c) in Eq. (38), there are seen to be contributions from poles in the upper half of the complex k plane at $K_{\omega} = k_F(1 + i\omega/\epsilon_F)^{1/2}$, at $iq^* = i(q_{TF} + \lambda)$ and at $i\lambda$. The calculation is straightforward although lengthy, so only the final result is given:

$$F_r(\epsilon_F + i\omega) = 8Z^* e^2 A \frac{2m}{\hbar^2} \left(\psi_r^{\mathrm{PW}}(i\omega) - \frac{2}{(1 + q_{TF}/2\lambda)^6} \psi_r^{\mathrm{core}}(i\omega) \right) \frac{1}{r} \; , \qquad (41a)$$

where

$$\psi_r^{\mathrm{PW}}(i\omega) = \frac{1}{(K_{\omega}^2 + q^{*2})^3} \left\{ e^{iK_{\omega}r} \left(K_{\omega}^2 + \frac{3iK_{\omega}}{r} - \frac{3}{r^2} \right) + e^{-q^*r} \left[\left(q^{*2} + \frac{3q^*}{r} + \frac{3}{r^2} \right) + \frac{1 + q^*r}{2} (K_{\omega}^2 + q^{*2}) + \frac{r^2}{8} (K_{\omega}^2 + q^{*2})^2 \right] \right\} \qquad (41b)$$

and

$$\psi_r^{\mathrm{core}}(i\omega) = \frac{\lambda^2}{(K_{\omega}^2 + \lambda^2)^4} \left\{ e^{iK_{\omega}r} \left(K_{\omega}^2 + \frac{3iK_{\omega}}{r} - \frac{3}{r^2} \right) + e^{-\lambda r} \left[\left(\lambda^2 + \frac{3\lambda}{r} + \frac{3}{r^2} \right) + \frac{1 + \lambda r}{2} (K_{\omega}^2 + \lambda^2) + \frac{r^2}{8} (K_{\omega}^2 + \lambda^2)^2 + \frac{r^3(K_{\omega}^2 + \lambda^2)^3}{48\lambda} \right] \right\} \; . \qquad (41c)$$

In order to appreciate Eqs. (40) and to motivate the procedure for numerical work, consider the limit of large r. From Eqs. (41) it is seen that

$$F_r(\epsilon_F + i\omega) \xrightarrow{r \to \infty} \tilde{F}_r(\epsilon_F + i\omega) = 8Z^* e^2 A \frac{2m}{\hbar^2} \left(\frac{K_{\omega}^2}{(K_{\omega}^2 + q^{*2})^3} - \frac{2}{(1 + q_{TF}/2\lambda)^6} \frac{\lambda^2 K_{\omega}^2}{(K_{\omega}^2 + \lambda^2)^4} \right) \frac{e^{iK_{\omega}r}}{r} \; . \qquad (42)$$

Since $K_{\omega} = k_F(1 + i\omega/\epsilon_F)^{1/2}$ gives exponential damping of the integrand in Eq. (40b) for $\omega > 0$, the leading term in $Q^{\sigma}(r)$ for large r is given correctly by using the approximation

$$K_{\omega} \simeq k_F(1 + i\omega/2\epsilon_F) \qquad (43)$$

in the phase of $e^{iK_{\omega}r}$ and setting $\omega = 0$ (i.e., $K_{\omega} = k_F$) elsewhere in the integrand. Thus (42) can be replaced by

$$\tilde{F}_r(\epsilon_F + i\omega) \simeq \frac{2m}{\hbar^2} (I_{dk_F} - J_{dk_F}) \frac{e^{ik_F r}}{r} e^{-ik_F r\omega/2\epsilon_F} \; , \qquad (44)$$

while Eqs. (14) and (15a) can be used to write

$$G_{dd}^{\sigma}(\epsilon_F + i0^+) = -e^{i\delta_d^{\sigma}(\epsilon_F)} \sin\delta_d^{\sigma}(\epsilon_F)/\Gamma_d(\epsilon_F) \; . \qquad (45)$$

Using these results in Eq. (40b) yields

$$Q^{\sigma}(r) \xrightarrow{r \to \infty} - \left(\frac{2m}{\hbar^2} (I_{dk_F} - J_{dk_F}) \right)^2 \frac{e^{i[2k_F r + \delta_d^{\sigma}(\epsilon_F)]}}{r^2}$$

$$\times \frac{\sin\delta_d^{\sigma}(\epsilon_F)}{\Gamma_d(\epsilon_F)} \int_0^{\infty} d\omega \, e^{-k_F r\omega/\epsilon_F} \; . \qquad (46)$$

The remaining integral is $\epsilon_F/k_F r$. From Eq. (26b) there finally results

$$Q^{\sigma}(r) \xrightarrow{r \to \infty} - \frac{\sin\delta_d^{\sigma}(\epsilon_F)}{r^3} \, e^{i[2k_F r + \delta_d^{\sigma}(\epsilon_F)]} \; , \qquad (47)$$

which when inserted in Eq. (40a) leads at once to Eq. (1).

For numerical work as well as for further developments in Sec. V, we found it useful to define a function $\chi^{\sigma}(r)$ by

$$Q^{\sigma}(r) = - \frac{\sin\delta_d^{\sigma}(\epsilon_F)}{r^3} \, e^{i[2k_F r + \delta_d^{\sigma}(\epsilon_F)]} \chi^{\sigma}(r) \; . \qquad (48)$$

From the above discussion of how various factors were simplified in the integrand of Eq. (40b) so as to yield Eq. (47), it is easy to see that

$$\chi^{\sigma}(r) = \frac{k_F r}{\epsilon_F} \int_0^{\infty} d\omega \left(\frac{F_r(\epsilon_F + i\omega)}{\tilde{F}_r(\epsilon_F + i0^+)} \right)^2 \frac{G_{dd}^{\sigma}(\epsilon_F + i\omega)}{G_{dd}^{\sigma}(\epsilon_F + i0^+)} \; . \qquad (49)$$

On measuring ω in units of ϵ_F and r in units of $1/k_F$, Eq. (49) provides a convenient dimensionless form for numerical work. The ω integral was evaluated by Simpson's rule with a variable mesh and also by Gaussian quadrature with an error control yielding accuracy of better than 0.1%.

This procedure was also followed for the finite-bandwidth (FBW) and the constant-self-energy[7]
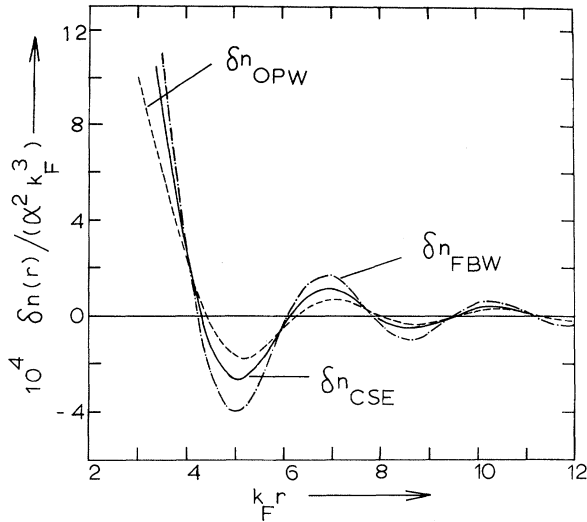
FIG. 5. Comparison of polarization per spin $\delta n^\sigma(r)$ for $Z_d^\sigma = 0.5$ in the OPW, FBW, and CSE models.

(CSE) models. In both of these cases, plane waves are used as a basis, so the appropriate $F_r(\epsilon_F + i\omega)$ is given by only the first term on the right-hand side of Eq. (41a). That is, the core orthogonalization term, Eq. (41c), is absent. In each case, $G_{dd}^\sigma(\epsilon_F + i\omega)$ is given by the analytic continuation into the upper half of the complex energy plane of the appropriate propagator defined in Sec. III. Furthermore, it is clear from the above analysis that the large-r limit, Eq. (47), and the general functional form of $\chi^\sigma(r)$, Eq. (49), also occur for the FBW and CSE models.

The computed $\delta n^\sigma(r)$ for these three models is shown in Fig. 5 for $Z_d^\sigma = 0.5$. It is important to note that the results for all three models are rather similar. In particular, there is agreement as to the sign of $\delta n^\sigma(r)$ at the first-nearest-neighbor distance, although the predicted magnitudes differ somewhat. Also, the relative phase and positions of nodes in $\delta n^\sigma(r)$ were found to be insensitive to variations in the parameter λ provided Z^* was chosen to maintain self-consistency in the sense of Sec. III. Corresponding changes in the magnitude of $\delta n^\sigma(r)$ near the nearest-neighbor distance were within 30%. The general consistency of these facts suggests that the phase or relative sign of $\delta n^\sigma(r)$ is given accurately by any of the present models, although uncertainty in the magnitude is of order 50% for small r. On the other hand, the asymptotic form, Eq. (1), differs in *sign* from our computed $\delta n^\sigma(r)$ in the neighborhood of the first nearest neighbor. This is illustrated in Fig. 6 for $Z_d^\sigma = 0.5$. We have carried out these calculations for Z_d^σ ranging from 0.5 to 4.5. In every case, the computed results for different models were in good agreement with each other but differed from the asymptotic

form, just as shown in Fig. 6, until $k_F r \gtrsim 10$.

From these results, it is possible to appreciate the important source of ω dependence in the integrand of $\chi^\sigma(r)$, Eq. (49). The ζ dependence of $\Sigma(\zeta)$ is not crucial, since the CSE model is in good agreement with the OPW and FBW models. In fact, it can be seen from calculations of $\Sigma(\zeta)$ in Sec. III that $|\partial\Sigma(\zeta)/\partial\zeta| \sim 0.1$ for $\zeta \simeq \epsilon_F + i0^+$. To check this, we calculated $\chi^\sigma(r)$ and $\delta n^\sigma(r)$ in an "s-wave" model in which the $\vec{k}$ dependence of $V_{\vec{k}dm}$ was neglected everywhere (thus only explicit ζ dependence of propagators was retained). The resulting $\delta n^\sigma(r)$ was very similar to the asymptotic form, Eq. (1), so it is not discussed at length. The result does show, however, that the explicit $\vec{k}$ and $\vec{k}'$ dependence of $T_{\vec{k}\vec{k}'}^\sigma(\zeta)$, which is reflected in the ζ dependence of the normalization constant ν_k.

It is evident that, owing to the extent of numerical work involved, these results are somewhat inconvenient, in their present form, for applications. In Sec. V, it is shown how an adequate interpolation formula can be developed.

V. INTERPOLATIONS FORMULA FOR $\delta n^\sigma(r)$

The fact that three different models give essentially the same numerical results for $\delta n^\sigma(r)$, even at nearest-neighbor distances, suggests that it may be feasible to develop an interpolation formula for $\delta n^\sigma(r)$. To do so in a simple and physical way, return to the complex quantity $\chi^\sigma(r)$ of Eq. (49) and write it in terms of its amplitude $\Lambda^\sigma(r)$ and phase $\theta^\sigma(r)$ by

$$\chi^\sigma(r) = \Lambda^\sigma(r)e^{i\theta^\sigma(r)} . \tag{50}$$
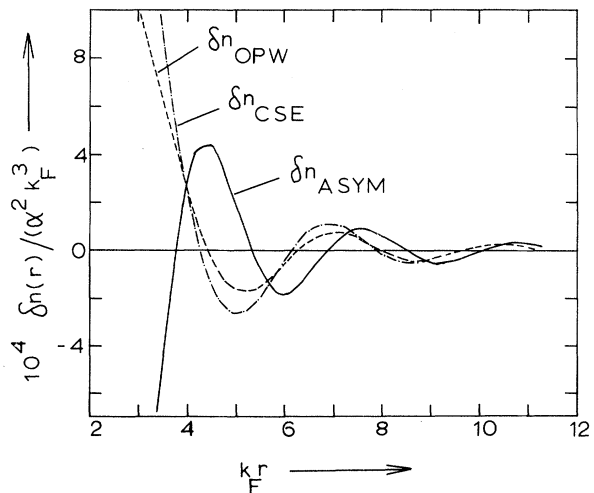
Use of the form in Eqs. (40) and (48) yields

FIG. 6. Comparison of the asymptotic form (denoted by ASYM) for $\delta n^\sigma(r)$ with results of OPW and CSE models for $Z_d^\sigma = 0.5$. The first-nearest-neighbor distance is given by $k_F a_{nn} \simeq 3$.

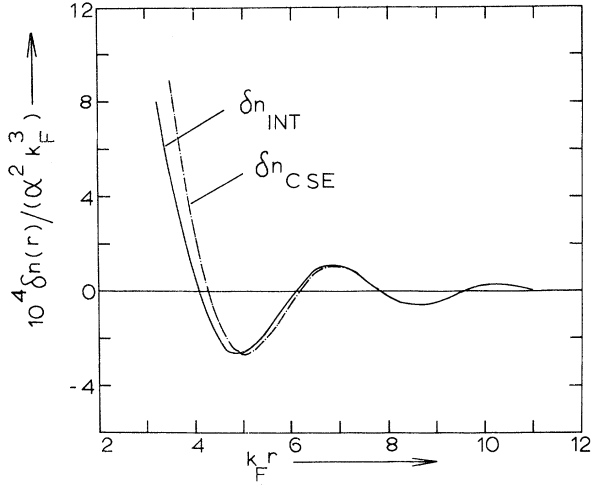FIG. 7. Comparison of the interpolation formula (denoted by INT) for $\delta n^\sigma(r)$ with results of the CSE model for $Z_d^\sigma = 0.5$.

$$\delta n^\sigma(r) = -\frac{5}{4\pi^2} \frac{\Lambda^\sigma(r)}{r^3} \sin\delta_d^\sigma(\epsilon_F)$$

$$\times \cos[2k_F r + \delta_d^\sigma(\epsilon_F) + \theta^\sigma(r)] \quad . \quad (51)$$

The chief advantage of this approach is that $\Lambda^\sigma(r)$ and $\theta^\sigma(r)$ are expected to show regular convergence to their asymptotic values of $\Lambda^\sigma(\infty) = 1$ and $\theta^\sigma(\infty) = 0$. They can then be approximated more easily than $\delta n^\sigma(r)$ itself, which is necessarily oscillatory.

To obtain an approximation for $\Lambda^\sigma(r)$ and $\theta^\sigma(r)$, we return to Eq. (49) to generate the leading correction terms to $\chi^\sigma(\infty) = 1$ in the expansion in powers of $1/k_F r$. Since all three models give very similar results, it will be adequate to consider only the simple CSE model. Thus the core orthogonalization term, Eq. (41c), will be dropped and the energy dependence of $\Sigma(\zeta)$ neglected. Furthermore, all exponentially decaying terms in Eq. (41b) can be dropped. The lowest-order corrections are thus obtained by using

$$\frac{F_r(\epsilon_F + i\omega)}{F_r(\epsilon_F + i0^+)} \simeq \left(\frac{k_F^2 + q^{*2}}{K_\omega^2 + q^{*2}}\right)^3 \left(\frac{K_\omega^2}{k_F^2} + \frac{3iK_\omega}{k_F^2 r}\right) e^{i(K_\omega - k_F)r}$$

(52a)

and

$$\frac{G_{dd}^\sigma(\epsilon_F + i\omega)}{G_{dd}^\sigma(\epsilon_F + i0^+)} \simeq \frac{\epsilon_F - E_d^\sigma + i\Gamma_d}{\epsilon_F - E_d^\sigma + i(\omega + \Gamma_d)} , \quad (52b)$$

where $E_d^\sigma = \epsilon_{d0}^\sigma + \Delta_d$ in Eq. (49). It is again a consequence of the exponential in Eq. (52a) that only small ω contributes to $\chi^\sigma(r)$ for large r. However, to obtain $\chi^\sigma(r)$ correctly to first order in $1/k_F r$, we must replace Eq. (43) by the more accurate higher-order expansion

$$K_\omega \simeq k_F \left(1 + \frac{i\omega}{2\epsilon_F} + \frac{\omega^2}{8\epsilon_F^2}\right) \quad (53)$$

for use in the exponential $e^{iK_\omega r}$. Also all first-order terms of the Taylor expansion in powers of ω of all other factors in the integrand must be included. On carrying out the expansions, Eqs. (52a) and (52b) become

$$\left(1 - \frac{3i\omega/\epsilon_F}{1 + q^{*2}/k_F^2}\right)\left(1 + \frac{i\omega}{\epsilon_F} + \frac{3i}{k_F r}\right) e^{-k_F r\omega/2\epsilon_F} e^{ik_F r\omega^2/8\epsilon_F^2}$$

and

$$1 - \frac{i\omega}{\epsilon_F - E_d^\sigma + i\Gamma_d} ,$$

respectively. Inserting these results in Eq. (49), we obtain

$$\chi^\sigma(r) \simeq \frac{k_F r}{\epsilon_F} \int_0^\infty d\omega\, e^{-k_F r\omega/\epsilon_F} e^{ik_F r\omega^2/4\epsilon_F^2}$$

$$\times \left(1 - \frac{6i\omega/\epsilon_F}{1 + q^{*2}/k_F^2} + \frac{2i\omega}{\epsilon_F} + \frac{6i}{k_F r} - \frac{i\omega}{\epsilon_F - E_d^\sigma + i\Gamma_d}\right) .$$

(54)

The integrals pose no problem, and the result, to first order, is

$$\chi^\sigma(r) = 1 + \frac{\gamma^\sigma + i\eta^\sigma}{k_F r} + O(r^{-2}) , \quad (55a)$$

where

$$\gamma^\sigma = -\frac{\Gamma_d \epsilon_F}{(\epsilon_F - E_d^\sigma)^2 + \Gamma_d^2} \quad (55b)$$

and

$$\eta^\sigma = \frac{17}{2} - \frac{6}{1 + q^{*2}/k_F^2} - \frac{\epsilon_F(\epsilon_F - E_d^\sigma)}{(\epsilon_F - E_d^\sigma)^2 + \Gamma_d^2} . \quad (55c)$$

The amplitude and phase of $\chi(r)$ are thus given by

$$\Lambda^\sigma(r) \simeq 1 + \gamma^\sigma/k_F r , \quad (56a)$$

$$\theta^\sigma(r) \simeq \eta^\sigma/k_F r . \quad (56b)$$

We have used these lowest-order approximations in Eq. (51) to define an interpolation formula. In Fig. 7, we compare the results of Eq. (51) for $Z_d^\sigma = 0.5$ with the complete numerical calculations given in Sec. IV for the CSE model. The agreement is seen to be good even near the first-nearest-neighbor distance. To some extent, this agreement is fortuitous, since at the nearest-neighbor distance, $\gamma^\sigma/a_{nn} \simeq -0.21$ and $\eta^\sigma/a_{nn} \simeq 3.4$, so that $\chi^\sigma(a_{nn})$ is very different from its asymptotic value of unity. However, the basic point is that the structure of the preasymptotic corrections can be used as a guide when obtaining trial estimates of $\theta^\sigma(r)$ and $\Lambda^\sigma(r)$. Of course, the resulting interpolation formula, Eq. (51), is no longer simply an expansion in powers of $1/k_F r$ and its ultimate justification is that it provides a good fit to the computed results. The simple approximations of Eqs. (56) were found to be adequate for $Z_d^\sigma \lesssim 1$ and for $Z_d^\sigma \gtrsim 4$, which is the expected range in physical applications. Alternative but more complicated in-

terpolation formulas can, of course, be obtained by straightforward procedures for the intermediate range of Z_d^σ, if desired.

VI. SUMMARY AND CONCLUSIONS

The spatial dependence of the polarization per spin produced in a free-electron metal by a magnetic ion has been calculated in the Friedel–Anderson picture. Three different models were used to describe the scattering of electrons by the impurity. Provided the resonance was described consistently, all three models led to essentially the same results for $\delta n^\sigma(r)$ even at the first-nearest-neighbor distance. On the other hand, the asymptotic form, Eq. (1), was found to be even of *opposite sign* in this range.

To simplify applications of the present results, an interpolation formula of convenient analytical form has been given. The application of these re-

sults to the calculation of hyperfine fields in alloys will be discussed elsewhere.

APPENDIX A: LOCALIZED-RESONANCE-STATE WAVE FUNCTION

As mentioned in Sec. II, the impurity resonance state is described by

$$\Phi_{dm}(\vec{r}) = \left(\phi_{dm}(\vec{r}) - \sum_{\vec{k}} B_{\vec{k}}(\vec{r}) \langle B_{\vec{k}}(\vec{r}) | \phi_{dm}(\vec{r}) \rangle\right) \nu_d ,$$

(A1)

where ν_d is the usual normalization constant,

$$\nu_d = \left(1 - \sum_{\vec{k}} |\langle B_{\vec{k}} | \phi_{dm} \rangle|^2\right)^{-1/2} .$$

(A2)

The overlap of the resonance state Φ_{dm} with the atomic state ϕ_{dm} is then

$$\langle \phi_{dm} | \Phi_{dm} \rangle = \left(1 - \sum_{\vec{k}} |\langle B_{\vec{k}} | \phi_{dm} \rangle|^2\right)^{1/2} .$$

(A3)

In order to evaluate the overlap integral in Eq. (A3), we shall study the term

$$\sum_{\vec{k}} |\langle B_{\vec{k}} | \phi_{dm} \rangle|^2 = \sum_{\vec{k}} \left| \int d^3r \frac{1}{\Omega^{1/2}} \left(e^{-i\vec{k}\cdot\vec{r}} - \sum_M b_{dM}^{(0)*}(\vec{k}) \Psi_{dM}^*(\vec{r}) \right) \phi_{dm}(\vec{r}) \right|^2$$

$$= \frac{1}{\Omega} \sum_{\vec{k}} \left| b_{dm}^*(\vec{k}) - b_{dm}^{(0)*}(\vec{k}) A_0 A \middle/ \frac{8(\lambda_0 + \lambda)^7}{45 \times 128} \right|^2 .$$

(A4)

The definitions of various quantities in Eq. (A4) are given in Sec. III. We may point out that the suffix 0 is used for the host metal and thus distinguishes host parameters from those of the impurity. Replacing the summation by integration in Eq. (A4), we get

$$\sum_{\vec{k}} |\langle B_{\vec{k}} | \phi_{dm} \rangle|^2 = \frac{2}{\pi} \int_0^\infty dk\, k^2$$

$$\times \left(\frac{a_{kd} - a_{kd}^{(0)}}{(\lambda_0 + \lambda)^7 / 128(\lambda_0\lambda)^{7/2}} \right)^2 . \quad (A5)$$

Since λ and λ_0 are close, we can write

$$\lambda_0 = \lambda(1 + \delta), \quad \delta \ll 1 . \tag{A6}$$

Using Eq. (A6) in Eq. (A5) and recalling the definition of a_{kd} from Eq. (23), it is easy to show that, to first order in δ,

$$a_{kd}^{(0)} = a_{kd} + a_{kd}\left(\frac{9}{2} - \frac{8\lambda^2}{\lambda^2 + k^2}\right)\delta . \tag{A7}$$

Substituting Eq. (A7) in Eq. (A5) and retaining terms to the lowest order in δ, we have

$$\sum_{\vec{k}} |\langle B_{\vec{k}} | \phi_{dm} \rangle|^2 \simeq \frac{2\delta^2}{\pi} \frac{8(48)^2}{45}$$

$$\times \int_0^\infty ds\, s^6\left(4.5 - \frac{8}{1+s^2}\right)^2 \middle/ (1+s^2)^8 . \quad (A8)$$

With $\delta = 0.2$, estimated from Cu and Mn $3d$ wave

functions, Eq. (A8) yields

$$\sum_{\vec{k}} |\langle B_{\vec{k}} | \phi_{dm} \rangle|^2 \simeq 0.08 . \tag{A9}$$

Thus the overlap in Eq. (A3) is

$$\langle \phi_{dm} | \Phi_{dm} \rangle \simeq 0.96 . \tag{A10}$$

This large overlap suggests the resonance state of the impurity ion can be approximated (within 4%) by the atomic-$3d$ wave function. This approximation considerably simplifies the algebra in the OPW model for resonant scattering.

APPENDIX B: ASYMPTOTIC FORMS OF δn_{Bd}^σ, δn_{dB}^σ, AND δn_{dd}^σ

In this appendix, we show that the contributions to the electron density as outlined in Eqs. (8a)–(8c) are negligible as compared to that in Eq. (8d). The analysis is based on the methods of Sec. IV.

$$\sum_m n_{B\,dm}^\sigma(\vec{r}) = \sum_m \sum_{\vec{k}} B_{\vec{k}}^*(\vec{r}) V_{\vec{k}\,dm}^* \int \frac{d\zeta}{2\pi i} \frac{G_{dd}^\sigma(\zeta)}{\zeta - \epsilon_k} f(\zeta)\phi_{dm}(\vec{r})$$

$$\simeq \alpha \sum_m \int \frac{d\zeta}{2\pi i} f(\zeta) F_r(\zeta) Y_{2m}^*(\hat{\vec{r}}) G_{dd}^\sigma(\zeta)\phi_{dm}(\vec{r})$$

(B1)

according to Eqs. (16b) and (37b). The m sum yields a factor $5/4\pi$ and the ζ integral can be transformed as in Sec. IV. Using the large r form for $F_r(\zeta)$ as given by Eqs. (44) and (45) for $G_{dd}^\sigma(\zeta)$, the asymptotic form of Eq. (B1) becomes

$$\sum_m \delta n^\sigma_{B\,dm}(\vec{r}) \xrightarrow[r\to\infty]{} -\frac{5\alpha}{4\pi^2} A r^2 e^{-\lambda r} \frac{2\epsilon_F}{k_F r^2} \frac{2m}{\hbar^2} (I_{dk_F} - J_{dk_F})$$

$$\times \frac{\sin\delta^\sigma_d(\epsilon_F)}{\Gamma_d(\epsilon_F)} \cos[k_F r + \delta^\sigma_d(\epsilon_F)] .$$

(B2)

The contribution of $\delta n^\sigma_{dm\,B}(\vec{r})$ is exactly the same as Eq. (B2). Using Eq. (22b) for A and Eq. (26b) for $\Gamma_d(\epsilon_F)$, the sum of Eqs. (8b) and (8c) is

$$\delta n^\sigma_{Bd}(r) = \sum_m [\delta n^\sigma_{B\,dm}(\vec{r}) + \delta n^\sigma_{dmB}(\vec{r})]$$

$$\xrightarrow[r\to\infty]{} -\frac{5\alpha}{2\pi^2} k_F^3 \left[\frac{32}{45}\left(\frac{\lambda}{k_F}\right)^7 \frac{\epsilon_F}{\Gamma_d(\epsilon_F)}\right]^{1/2}$$

$$\times \sin\delta^\sigma_d(\epsilon_F) e^{-\lambda r} \cos[k_F r + \delta^\sigma_d(\epsilon_F)] .$$

(B3)

The contribution of Eq. (8a) is given for any r by

$$\delta n^\sigma_{dd}(r) = \frac{5}{4\pi} A^2 r^4 e^{-2\lambda r} .$$

(B4)

Of course, the well-known asymptotic form of Eq. (8d) is

$$\delta n^\sigma_{BB}(r) \xrightarrow[r\to\infty]{} -\frac{5\alpha^2}{4\pi^2 r^3} \sin\delta^\sigma_d(\epsilon_F) \cos[2k_F r + \delta^\sigma_d(\epsilon_F)] .$$

(B5)

Typical parameters for systems of the CuMn type are $k_F \sim 1$ Å^{-1}, $a_{nn} \sim 3$ Å, and $\lambda \sim 5$ Å^{-1}. Using these values in Eqs. (B3)–(B5) yields the estimates

$$k_F^{-3} \delta n^\sigma_{dd}(a_{nn}) \sim 8.4 \times 10^{-9} ,$$

$$k_F^{-3} |\delta n^\sigma_{Bd}(a_{nn})| \lesssim 0.5\alpha \sin\delta^\sigma_d(\epsilon_F) \times 10^{-4} ,$$

and

$$k_F^{-3} |\delta n^\sigma_{BB}(a_{nn})| \lesssim 0.5\alpha^2 \sin\delta^\sigma_d(\epsilon_F) \times 10^{-2} .$$

(B6)

It is seen that δn^σ_{dd} and δn^σ_{Bd} are orders of magnitude smaller than δn^σ_{BB}. These estimates are based on using asymptotic forms even as close as the first-nearest-neighbor distance, but these are quite adequate for obtaining relative orders of magnitude.

---

[1]E. Daniel and J. Friedel, in *Proceedings of the Ninth International Conference on Low-Temperature Physics*, edited by J. G. Daunt, D. O. Edwards, F. J. Milford, and M. Yaqub (Plenum, New York, 1965).

[2]A. Blandin, in *Theory of Magnetism in Transition Metals*, edited by W. Marshall (Academic, New York, 1967).

[3]P. W. Anderson, Phys. Rev. **124**, 41 (1961).

[4]N. Rivier and J. Zitkova, Advan. Phys. **20**, 143 (1971).

[5]P. W. Anderson, in Ref. 2.

[6]The parameters λ for Cu and Mn $3d$ wave functions were taken from J. B. Mann, *Atomic Structure Calculations*, Los Alamos Scientific Laboratory, University of California, Los Alamos, N. Mex., 1968 (unpublished).

[7]D. J. W. Geldart, Phys. Letters **38A**, 25 (1972).

Magnetic Susceptibility Measurements of the Spin-$\frac{1}{2}$ Linear-Chain α-*bis*-(N-Methylsalicylaldiminato)-Copper (α-CuNSal)†

Robert C. Knauer and R. R. Bartkowski
Sandia Laboratories, Albuquerque, New Mexico 87115
(Received 16 June 1972)

The susceptibility of the spin-$\frac{1}{2}$ linear chain α-CuNSal has been measured by the Faraday-balance technique from 2–300 K. The measurements over the entire range can be understood in terms of several approximations applicable to the high- or low-temperature regimes of the Heisenberg linear chain. From these models the nearest-neighbor-exchange strength has been obtained by two different techniques and its value determined to be $J/k = -3.2 \pm 0.2$ K. The excellent fit of the magnitude and temperature dependence of the data to these approximations over this wide temperature range confirms the one dimensionality of the system and yields an accurate measurement of the exchange constant.

INTRODUCTION

X-ray crystallography studies[1,2] have shown that α-*bis*-(N-methylsalicylaldiminato)-copper (α-CuNSal) is highly one dimensional in structure with a Cu-Cu separation of 3.33 Å along the chain or c axis and a minimum distance between chains of 9.19 Å. Electron-spin-resonance- (ESR) line-

shape experiments[2,3] indicate that the exchange interaction between non-nearest-neighbor Cu atoms is small compared to nearest-neighbor exchange coupling. Previously, the classic spin-$\frac{1}{2}$ linear-chain system $Cu(NH_3)_4SO_4 \cdot H_2O$ has been shown,[4] on the basis of magnetic-susceptibility and specific-heat data, to agree with the calculations of Bonner and Fisher[5] (BF) for a spin-$\frac{1}{2}$ one-dimen-